Journal of Materials Chemistry

Dynamic Article Links ►

Cite this: DOI: 10.1039/c0xx00000x

ARTICLE TYPE

www.rsc.org/xxxxxx

Mesoporous Titanium Dioxide Films Using Partially Fluorinated Surfactant Templates in Ethanol

Adrian M. Hawley,[a,b] Karen J. Edler*[a] and Stephen J. Roser[a]

Received (in XXX, XXX) Xth XXXXXXXXX 20XX, Accepted Xth XXXXXXXXX 20XX

DOI: 10.1039/b000000x

Mesoporous titanium dioxide films have been produced via a self assembly pathway at the air-ethanol interface using partially fluorinated surfactants as structure directing agents. The high level of surface activity displayed by partially fluorinated compounds in alcohols has been used to generate an ordered film at the air-solution interface, as titanium oligomers condense into an ordered inorganic network. The minimisation and exclusion of water in these preparations directs structure formation at the interface and slows the titania polymerisation. X-ray scattering and Brewster angle microscopy techniques have been used to study the formation and structure of these materials.

Introduction

Since the development of the MCM family of materials in the early 1990s, mesoporous materials have represented an active area of research.[1] These materials have generated interest for application in such diverse fields as catalysis, gas storage and photovoltaics among other areas.[2, 3] Although powdered materials are useful, the production of mesoporous films provides additional potential for application or improved efficiency in the fields of coatings, sensors and solar cell technology.[4-6]

The use of surface active molecules as structure directing agents to form mesostructured materials has grown in diversity in recent years.[1] A range of self assembly pathways using a variety of surfactants, polymers and inorganic precursors have now been developed and this continues to expand.[2] Within the range of structure directing agents used, fluorinated and partially fluorinated molecules represent an area of research growth in recent years due to their differences from hydrogenous molecules. Properties such as increased chain rigidity give rise to surface activity in a wide range of media, including alcohols, and critical micelle concentrations much lower than those of hydrogenous surfactants.[7-9] Fluorinated surfactants have found use in preparation of mesostructured silica powders and films and have also been used to form mixed titania–silica materials.[10-12]

The formation of surfactant-templated films has so far been dominated by evaporation assisted self assembly (EISA). In EISA an ultra-dilute solution of surfactant and inorganic precursor in a volatile solvent is applied to a substrate by dip or spin coating, resulting in a film a few hundred nm thick.[13] This method can provide highly ordered coatings but is severely dependent upon tight control of the temperature and relative humidity during deposition and aging making it difficult to reproduce especially for large areas. As an alternate route, providing free-standing mesostructured membranes the growth of films at solution interfaces is attractive, since it is much less influenced by ambient conditions, is easily scalable to large areas and, for silica, can provide thicker films without multiple coatings. However, for species other than silica, including titania, film growth at solution interfaces is much less developed. Earlier work by Henderson et al[14, 15] demonstrated formation of lamellar TiO_2 films templated by anionic surfactants on aqueous solutions, however these were too thin to recover from the interface for calcination or other studies. Our earlier work has demonstrated that an ethanolic solution can be used to control reactions between titania and a templating block-copolymer, allowing film formation.[16] Here we build on this by studying commercially-available fluorinated surfactants as templates. These species form micelles in ethanol more readily than hydrogenous block copolmers and provide potential for tailoring the template by varying the amphiphile properties using commercially available materials.

The ability to use non-aqueous reaction conditions provides an opportunity to control formation of inorganic materials. Inorganic precursors, especially transition metal precursors such as alkoxides, tend to be highly reactive toward hydrolysis and condensation and control of these reactions is key to generating ordered mesostructured materials. Rapid condensation leads to powders rather than films and incomplete hydrolysis leads to flaws in final materials.[17, 18] Although fluorinated surfactants have been successfully used to form ordered silica mesostructures in the past, the extension of these methods to both pure titania materials and non-aqueous environments is reported here for the first time. This development holds considerable significance for the development and application of mesoporous materials as it shows that different formation pathways exist, that may be more suitable for some applications, especially given that the method used here is both straightforward and highly reproducible.

Experimental

The partially fluorinated surfactant FSO-100, average structure $F(CF_2CF_2)_4(CH_2CH_2O)_9H$, (average molecular weight 725 g mol^{-1}) was kindly provided by DuPont de Nemours. The as-received inhomogeneous surfactant was centrifuged at 11000 rpm and 15°C for 60 min and the golden brown liquid major fraction separated for use in film formation, while solid impurities were discarded. Analytical reagent grade HCl (37% w/w) and AR-grade (99.8% pure) anhydrous ethanol were purchased from Fisher Scientific, and titanium (IV) butoxide $Ti(OBu^n)_4$ (99% w/w) was purchased from Acros Organics.

Films were prepared by dissolving FSO-100 (2.25 mMol) in ethanol (434 mMol). HCl (14.9 mMol) was added to $Ti(OBu^n)_4$ (2.00 mMol) in a separate glass vial and agitated to achieve a yellow liquid. This yellow phase was added to the ethanol-surfactant solution, to give a solution with overall mole ratios of 0.52 FSO-100 : 100 CH_3CH_2OH : 3.43 HCl : 11.86 H_2O : 0.46 $Ti(OBu^n)_4$. This solution, the standard film preparation, was stirred for a further 30s before the initially clear, almost colourless solution was poured into a dish and allowed to stand at room temperature. A colourless, transparent film formed within one hour as yellow colour developed in the solution. Where required, solid films were recovered after 24 hrs onto microscope slides or open plastic mesh with 1cm holes, raised slowly through the interface to collect the film. Reagent concentrations were varied in the ranges 1.13 – 3.87 mMol FSO-100; 3.8–18.6 mMol HCl and 0.07–3.37 mMol $Ti(OBu^n)_4$. In addition the effect of water was studied in the range 6.56–41.33 mMol and a completely non-aqueous preparation was made without acid.

Growth of films at the air-liquid interface was observed using a Nanofilm Technologies Nanoscope Elli2 Brewster Angle Microscope (BAM). BAM images of the surface of reaction solutions in a 6cm diameter Petrie dish were taken at 5min intervals during and after film formation. Film formation was judged to occur when a previously moving surface became stationary. These films were collected for further analysis after ~24hrs of growth. To find limiting film formation conditions and determine whether ethanol evaporation drives film formation, preparations at double the ethanol volume were studied. The solution mass was monitored on a microbalance and film growth observed by BAM. No film formed until half the mass had evaporated, so subsequent preparations used the standard ethanol volume.

Formation of mesostructure in films at the air-solution interface was studied using time resolved off-specular reflectivity and specular reflectivity at the Troika II beamline at the ESRF,[19] using X-rays of wavelength 1.546Å. Solutions were placed in Teflon troughs, 152×42 mm, which hold 20-30 mL of liquid thermostatted at 25°C. Time-resolved off-specular experiments followed growth of the films at 1min intervals with an X-ray incident angle of 1.27° giving a range of 0–0.23 $Å^{-1}$ in Q_Z ($Q_Z = (4\pi\sin\theta)/\lambda$). Full details of this technique have been previously reported.[20] Film formation was deemed to have occurred when specular reflectivity was lost due to increasing surface roughness caused by film formation, as the development of new peaks from the film mesostructure was inconsistent. Specular reflectivity patterns from the films were subsequently collected in the range 0–2.5°, and fitted using a layer model in the program MOTOFIT[21] written in Igor Pro (Wavemetrics). A neutron reflectivity pattern of a titania film from a standard preparation was also taken on the SURF reflectometer[22] at the ISIS Spallation Neutron Source, Rutherford Appleton Laboratory to provide more structural information. An incident angle of 1.5° was used to collect data between 0.048-0.613 $Å^{-1}$ in Q_Z. The film was grown at 25°C in the same trough used for X-ray reflectivity, on a subphase of 65mol% C_2D_5OD, 35mol% C_2H_5OH, and data fitted using MOTOFIT, as for X-ray reflectivity.

Small Angle Neutron Scattering (SANS) from solutions of FSO-100 in d6-ethanol with $Ti(OBu^n)_4$ at 1-5 times the concentration of the standard preparation was measured on LOQ at ISIS.[23] An Anton Paar SAXSess instrument (λ=1.54 Å) with an angle range of 0.0077–2.70 $Å^{-1}$ was used for small angle X-ray scattering (SAXS) measurements. Dry solid films were ground into a powder which was held between pieces of sticky tape. Films on microscope slides were calcined at 600°C in air before material was scraped from the slides and mounted in tape in a solid sample holder. SAXS measurements of FSO-100 solutions in ethanol were made in a 1mm diameter quartz capillary. An ethanol background in the same capillary was subtracted from the data and corrections made for beam shape. Data was fitted to models of ellipses or polydisperse spheres using the NIST SANS analysis software[24] written for Igor Pro.

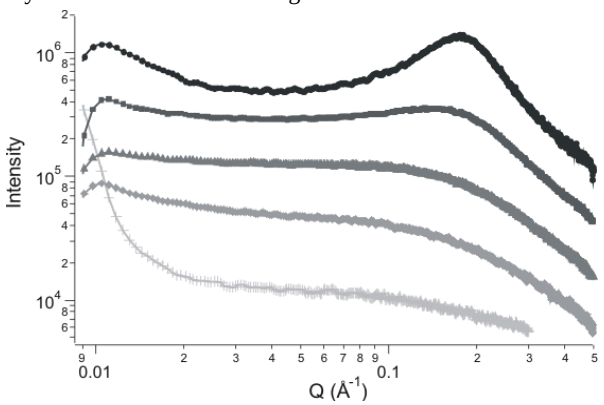

Fig 1 SAXS profiles of FSO-100 surfactant in ethanol. Patterns corresponding to 10% (crosses), 20% (diamonds), 40% (triangles), 60% (squares) and 80% (circles) wt. are shown.

TEM images were taken using a JEOL 1200 EX microscope operated at 120 kV. Calcined film material was scraped off a microscope slide and the powder dispersed into isopropanol via sonication prior to mounting on a copper TEM grid. SEM images were collected on a JEOL JSM6480LV with an operating voltage of 20 kV. Films were recovered onto microscope slides, calcined and sputter coated with gold prior to imaging to prevent charging or measured by scraping film off the substrate after calcination and mounting on carbon tape on an aluminium stub. Quantitative elemental analysis was performed by EDX in both SEM and TEM to ensure the nature of the material in the image corresponded to titania film material. No evidence of residual fluorine was detected in EDX in SEM down the the resolution limit of the instrument (0.1wt%). Thermogravimetric analysis (TGA) was carried out using a Perkin Elmer TGA 7, heating from 25 °C to 600 °C at a rate of 1.0 °C/min. A film was grown at standard concentration, recovered from solution on a microscope slide and dried for 24 hrs before the TGA measurement.

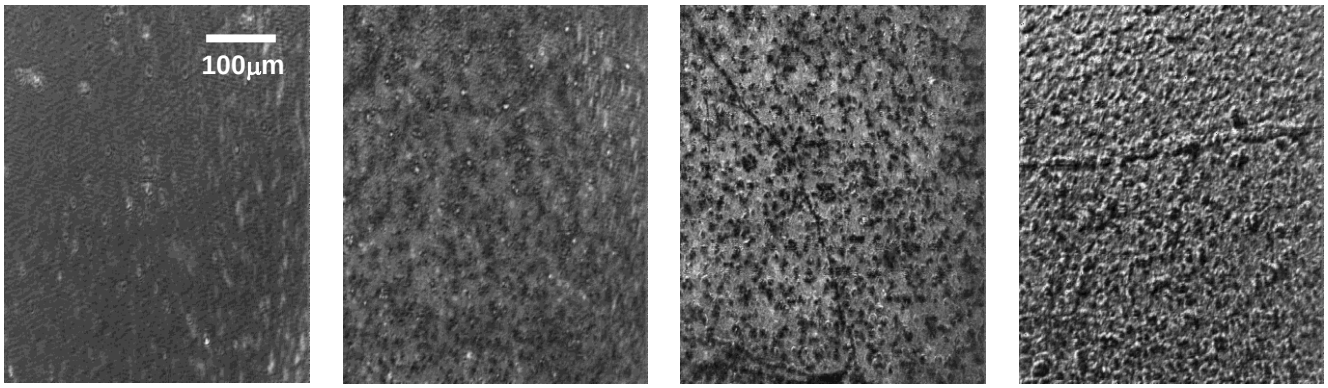

(a) *(b)* *(c)* *(d)*

Fig 2 Brewster angle microscope images of a film developing at the air-ethanol interface. Image (a) shows the surface directly after solution mixing while images (b), (c) and (d) show the surface after 160 minutes, 305 minutes and 26 hours respectively.

Table 1: Summary of SAXS models for FSO-100 surfactant in ethanol. R_a is the rotation axis of ellipsoids or the radius of a sphere as appropriate, R_b is the minor axis of ellipsoids and PD is the Schulz polydispersity of the sphere radius.

FSO-100 (% wt.)	Micelle Shape	R_a (Å) ± 2	R_b (Å) ± 2	PD ± 0.05
10	Spherical	11	-	0.18
20	Spherical	10	-	0.10
30	Spherical	10	-	0.27
40	Ellipsoidal	10	9	-
50	Ellipsoidal	18	10	-
60	Ellipsoidal	30	10	-
70	Ellipsoidal	37	10	-
80	Ellipsoidal	35	10	-
90	Ellipsoidal	38	10	-

A nitrogen adsorption isotherm for powdered, calcined films was measured on a Micromeritics Accelerated Surface Area and Porosimetry Analyzer (ASAP) 2010 instrument. Material, calcined in air at 600°C, from 30 films made with identical reagent concentrations, was combined to provide a representative and sufficiently large sample (approximately 0.1g). The sample was degassed under vacuum overnight above 400°C before measurement at 77 K over a partial pressure cycle of 0 – 1 – 0 in 0.03 increments with an equilibration period of 45s at each partial pressure. The specific surface area calculated using the BET method applied to the adsorption branch.

Results

FSO-100/Ethanol Subphase Solutions

To improve understanding of the subphase during film formation, solutions of 0 to 90wt% FSO-100 in ethanol were studied by SAXS, *Fig 1*. Data for all concentrations was modelled with spherical, ellipsoidal, cylindrical and lamellar models using a hard sphere structure factor. The best model results (assessed by minimum χ^2 values from fitting) are shown in Table 1.

No structure is apparent in solutions at low FSO-100 content, but from 10wt% to 40wt% the data may be fitted by isolated spherical micelles of 20Å diameter. This apparently small size is due to a lack of contrast between the polyethylene oxide chain of the surfactant and the ethanol solvent leaving the 8-carbon fluorinated section of FSO-100 as the main contributor to the scattering. At concentrations above 70wt% modelling suggests the surfactant forms prolate ellipsoids with diameters approximately 72 x 20 Å. A peak at Q = 0.177 $Å^{-1}$ developed in the scattering patterns at this point due to hard sphere interactions between micelles. Between the two extremes, 40wt% - 70wt%, FSO-100 micelles become more ellipsoidal as the concentration increases. The 10wt% sample is closest to the film forming solutions, which used 7.5wt% surfactant.

Film Development

Titania films forming at the air-liquid interface were studied using Brewster angle microscopy and time-resolved off-specular X-ray reflectivity. BAM images showed that when film precursors are initially mixed, a uniform black surface is observed which is disrupted by swiftly moving bright specks due to surfactant migration to the interface (*Fig 2a*). BAM images for a standard film preparation noted little change until formation of a stationary surface indicative of film formation 160 min after the addition of the $Ti(OBu^n)_4$, *Fig 2b*. As the film forms, the subphase solution becomes yellow, associated with formation of titanium oxide oligomers in previous reports of film preparations.[14, 15] Further development of structure at the interface leads to an optically clear film after a further hour with additional surface structure becoming visible in BAM images. At this point *Fig 2c*, fractures could be observed in the film if it had been damaged by agitation when aligning the microscope. Films continued to grow over more than a day, becoming visible by eye and with BAM showing an increasingly rough interface, *Fig 2d*, including areas with the appearance of holes arising from distortion of the top layers of film due to contraction as the surface dries and titania condensation continues.

The transition from a mobile to a stationary interface was used to study the effects of different reagent concentrations on the film formation time. *Fig 3a* shows formation times as the concentration of $Ti(OBu^n)_4$ was varied. Unusually, the film formation time increases as the amount of $Ti(OBu^n)_4$ increases, with formation time almost doubling from 55 min for 0.15 mMol of $Ti(OBu^n)_4$ to 90 min at 2.85 mMol. At the lowest concentration, 0.07 mMol, only a partial film formed and below this concentration no film is visible. In contrast, at the highest concentration studied, 3.37 mMol, film formation was difficult to determine as the mobile to stationary transition was unclear. As a result, there is greater uncertainty in these times.

Although limiting the concentration of titania precursors

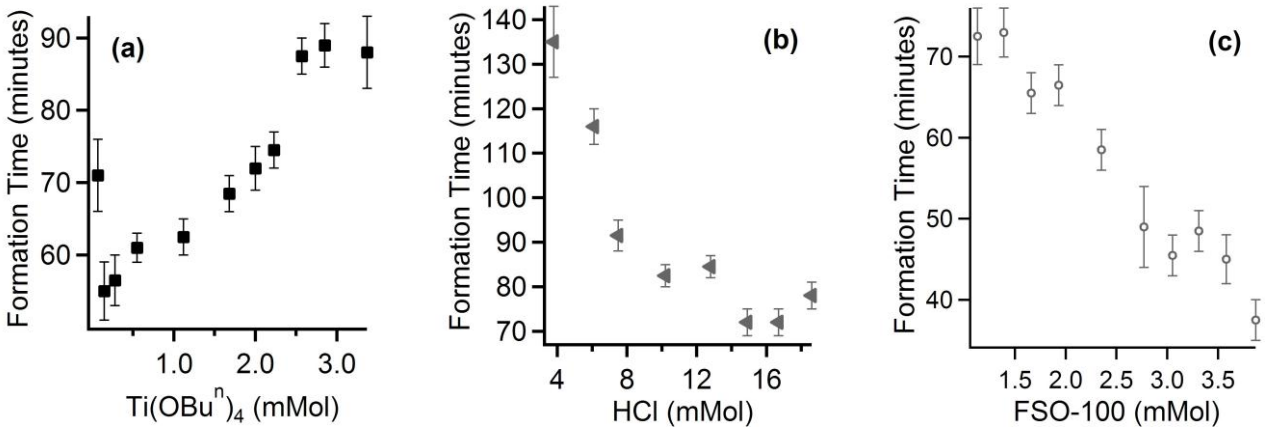

Fig. 3: Film formation times observed for changes in (a) Ti(OBu^n)$_4$ (b) HCl and (c) partially fluorinated surfactant, FSO-100, concentration

normally controls and slows formation of inorganic material,[2] the opposite trend is observed here. We suggest that the low water content, only present in the acid added to the reaction mixture, causes water availability to be the limiting factor in the time for film formation. Limiting the availability of water to control inorganic polymerisation has been reported in the past and is expected to be operating here.[25, 26] It is also recognised that, in a non-aqueous preparation, atmospheric moisture can provide water for titania hydrolysis and it is likely that this contributes to film formation at the air-solution interface.[2, 27]

The limiting effect of water is supported by the results from changing HCl concentration, *Fig 3b*. As HCl concentration increases, the film formation time is reduced from 135 minutes when 3.8 mMol of HCl is used to 78 minutes for 18.6 mMol. A film also forms at the interface within two hours when no acid, and consequently no water, is added to the solution at all; to our knowledge the first time this has been observed. As the use of highly acidic reaction conditions is a well-established method for the control and slowing of inorganic polymerisation reactions, these results are counter-intuitive.[2] However, in the context of water being a limiting factor in film formation the increase in water content, present as 63wt% of the HCl, allows more rapid film development, outweighing the inhibiting effect of higher acid concentration. Furthermore, formation of a film without any acid suggests that the acid itself is playing a relatively minor role.

Data displayed in terms of the relative molar ratio of H_2O to Ti(OBu^n)$_4$ shows good agreement between the two series of experiments, (*Fig 4)*. There is a steep decline in formation time as the water content increases before levelling off once the H_2O : Ti(OBu^n)$_4$ ratio is approximately 45 or higher. Experiments conducted with additional water added to the reaction mixture also show a reduction in formation time at higher water contents and although these points do not lie directly over those in HCl and Ti(OBu^n)$_4$ variation experiments, this trend supports the proposed idea. For complete hydration of the inorganic precursors a stoichiometric ratio of four to one, water to titanium, is adequate,[28] however it seems that a considerably greater ratio is required before the water becomes sufficiently freely available for reaction that it is no longer a limiting factor in the film formation time. Furthermore, when water content has been used as a controlling mechanism in the past it has been at lower molar ratios than used here.[25, 28] In our case, once a ratio of 45:1 is achieved the availability of water no longer limits film formation but below this level it is the most important consideration.

Varying FSO-100 surfactant concentration *Fig 3c* gives a decrease in formation time from 73 min at a concentration of 1.13 mMol FSO-100 to 37 min when 3.87 mMol of surfactant is used, representing a halving of the formation time. This shows a similar dependence upon the surfactant concentration for film formation to that seen for aqueous silica-based systems templated with non-ionic surfactants.[29] This trend is also observed in formation times from X-ray reflectivity experiments (discussed below). However, unlike the silica systems, if the data from Ti(OBu^n)$_4$ and FSO-100 variation experiments are combined to compare the effects of the Ti:FSO-100 molar ratio, no overall trend is observed. This suggests that this ratio is not a dominating factor in this titania system (data not shown).

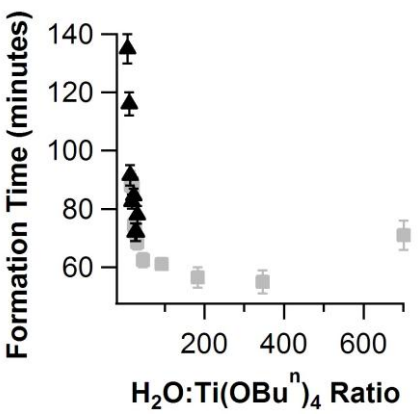

Fig. 4: Variation of film formation time with respect to H_2O to Ti(OBu^n)$_4$ molar ratio. Data combined from HCl, black triangles, and Ti(OBu^n)$_4$, grey squares, variation (see Fig. 3a,b).

Time-resolved off-specular X-ray reflectivity measurements showed concordant trends for formation time with reagent concentration, however, all formation times were lower than in BAM experiments. The larger surface area of the troughs used in these experiments compared to the petrie dishes used for BAM is the probable source of this difference as it facilitates greater access to atmospheric moisture and greater evaporation leading to

more rapid development. Similar effects have been seen in silica film growth experiments.[29] The ambient relative humidities and sample temperatures in the laboratory and at the ESRF were recorded during experiments and were similar. *Fig 5* shows the off-specular reflectivity typically observed during film growth. The specular reflectivity peak is initially present (at Q = 0.18 Å^{-1}) but decays and is then lost during film development. An initially broad diffraction peak gradually develops and becomes sharper close to the specular peak position, accompanied by growth of a Yoneda wing (at 0.017 Å^{-1}) due to increasing surface roughness after film formation. Peak positions for samples at different concentrations observed in the time-resolved data are identical to those discussed below for the final film structures.

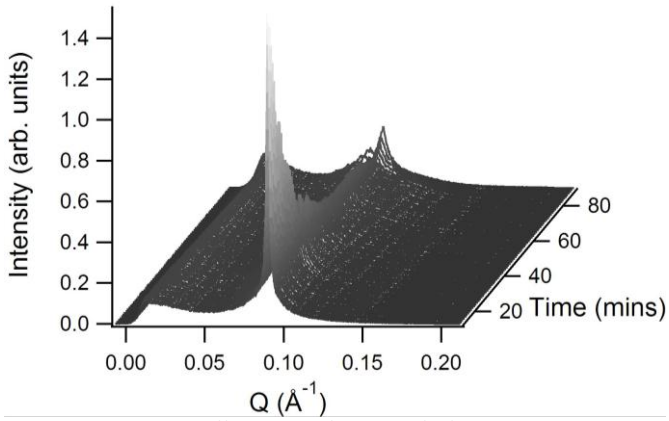

Fig. 5: Time-resolved off specular reflectivity of a film developing at the air-solution interface from a film forming solution at 2.85mM Ti(OBu^n)$_4$ with standard concentrations of other reagents.

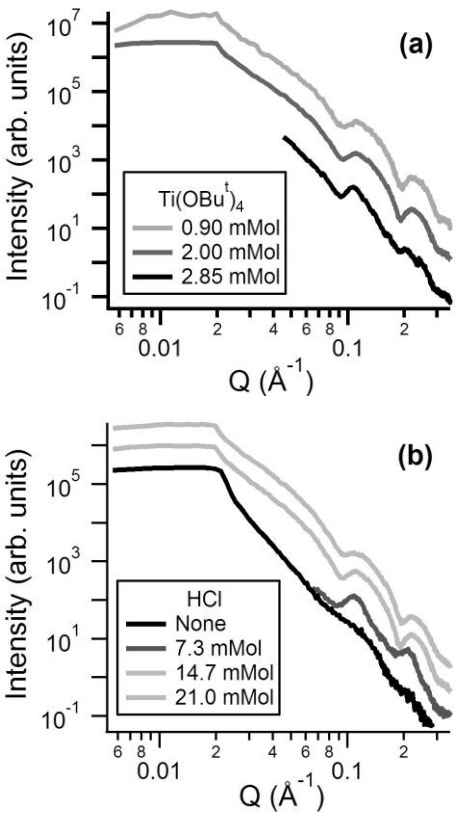

Fig. 6: X-ray reflectivity profiles of films at the air-solution interface showing variation with (a) Ti(OBu^n)$_4$ and (b) HCl concentration. Data is offset for clarity.

These X-ray reflectivity experiments show no structure at the interface prior to film development and SANS experiments on Ti(OBu^n)$_4$/FSO-100/ethanol solutions at film forming concentrations also show a lack of structure (data not shown), so no liquid crystal or coacervate phase exists in the subphase. The structured film therefore develops from a dilute disordered micellar solution, growing progressively at the interface after an initial induction period where little change at the surface is noted. Such a mechanism is expected to be diffusion-limited and higher concentrations of Ti(OBu^n)$_4$ and surfactant should afford more rapid film formation. However, the availability of water limits film formation by limiting inorganic polymerisation, causing the induction period. In silica systems and film forming systems containing organic polymers with surfactant, oligomers of sufficient molecular weight are required before film formation occurs[30] and it appears that this also plays a role in formation of these titania films ie a certain degree of titania polymerisation is required before film formation occurs.

The data for reagent variation and film growth show that the relative concentrations of water and Ti(OBu^n)$_4$ are of key importance to film formation time. In preparing the films, the acid is initially mixed with titanium butoxide to form a homogeneous solution, before adding it to the surfactant solution. The Ti(OBu^n)$_4$ is completely hydrolysed prior to addition to the surfactant solution as, if this were not the case, variation of time prior to mixing these solutions would be expected to lead to variation in formation times, but this is not observed. As the titania precursor is fully hydrolysed it is not immediately clear why the water:Ti ratio should be so important as subsequent condensation is not expected to be inhibited by lack of water. This is discussed further below, considering the evolving structure of the films.

Final film structure

The structure of films after ~90min growth at the air-water interface was studied by X-ray and neutron reflectivity (*Fig 6, Fig 2S supplementary materials)*. Solution evaporation during film growth and subsequent interference of the PTFE trough at low angles led to a reduction in the angle range studied. From titania precursor variation experiments, the most highly structured films, with the most well developed peaks, are those that have a low Ti(OBu^n)$_4$ concentration. A low acid concentration also appears to improve ordering in the film but some acid is required for high levels of structure to form. The majority of the scattering patterns correspond to a lamellar structure with peak positions and *d*-spacings displayed in *Table 2*.

One exception to the lamellar phase is found in preparations with no acid. In this case the scattering profile is poorly resolved and although a peak is present, no firm structure determination was possible. A lower acid concentration may reduce interactions between the surfactant and titania precursors, reducing ordering and inhibiting formation of a structured film as a result. Reduced ordering was also noted at the highest Ti(OBu^n)$_4$ concentrations where acid:titania ratios are also low, giving equivalent results.

Fitting of the data in *Fig 6* to a layered model suggested that the films consist of an initial FSO-100 layer at the solution

Table 2: Peak and shoulder positions and interlayer spacings calculated for $Ti(OBu^n)_4$ and HCl variation in film preparations.

$Ti(OBu^n)_4$ Concentration	Peak/Shoulder Positions ±0.002 ($Å^{-1}$)		*d*-spacing ±4 (Å)
0.90 mMol	0.112	0.225	56
2.00 mMol	0.110	0.220	57
2.85 mMol	0.105	0.201	60
HCl Concentration	Peak/Shoulder Positions ±0.002 ($Å^{-1}$)		*d*-spacing ±4 (Å)
No Acid	-	-	-
7.3 mMol	0.109	0.211	58
14.7 mMol	0.110	0.222	57
21.0 mMol	0.113	0.221	56

surface, with up to six well-ordered alternating layers of TiO_2/ethylene oxide/solvent (36±2Å) and fluorosurfactant tails (20±2Å) forming underneath. Beneath this is a large region of disordered micelles and titania species in solvent (which correspond to the final film structures observed by SAXS and TEM below). Since SEM images (*supplementary materials, Fig 1S*) suggest the films are ~3 microns thick after calcination, the highly ordered surface layers form only a small part of the total film structure. The reflectivity patterns were also recorded at relatively short film growth times, since films were not havested until 24 hrs after initial solution mixing. Increasing surface roughness (eg *Fig 2d*) makes reflectivity from later stages of film growth impossible, thus films harvested after film growth is complete are likely to have a less ordered structure than the initially formed layers at the interface.

Neutron and X-ray reflectivity patterns recorded at a similar times after a standard solution was poured into the trough, were fitted to the model described above (*supplementary materials Fig 2S, Table 1S*). Assuming that one layer contains only the fluorinated tails of the surfactant, with equivalent properties to perfluorooctane, the scattering length densities derived from model fitting can be used to calculate the TiO_2/ethyelene oxide/solvent content in the other layer. From this analysis the hydrophilic layers contain very little solvent, and are largely TiO_2 (~40±7mol%) and ethylene oxide (~60±7mol%).

After growth, films were easily recovered from the interface on a plastic mesh with ~1cm wide holes, or on a substrate such as a clean microscope slide raised slowly from beneath the film. Little residue remained when the remaining subphase was allowed to evaporate. Calcination at 600°C caused free-standing films to crack but films on substrates retained their integrity. Since HF is highly volatile, residue from the fluorosurfactant template was not expected to remain within the films. This was confirmed by EDX measurements which showed no evidence of fluorine on the surface or fractured edges of the film. Further study of dry films recovered from the air-liquid interface was carried out using TGA, SAXS and TEM.

TGA indicates that a film dried for 24 hrs under ambient conditions contained ~11wt% solvent (mass lost at ~120°C and below, attributed to n-butanol, ethanol and water), 80wt% surfactant and 9wt% TiO_2 which remained after heating to 600°C. This is equivalent to a molar ratio of 1 FSO-100 : 0.95 TiO_2, which corresponds well to the initial molar ratio used in the standard synthesis where 1 FSO-100: 0.88 $Ti(OBu^n)_4$ was used.

SAXS patterns from powdered films after calcination show evidence of retained mesopores. There are no significant differences in the film structures when the concentration of HCl or FSO-100 are changed (data not shown). However, when the concentration of $Ti(OBu^n)_4$ is increased the SAXS patterns develop a shoulder around Q = 0.082 $Å^{-1}$, *Fig 7*. These patterns suggest that the films have a porous structure of either ellipsoidal titania particles or ellipsoidal holes within the titania formerly occupied by surfactant, with the latter more likely when compared with TEM images of the materials (*Fig 8*).

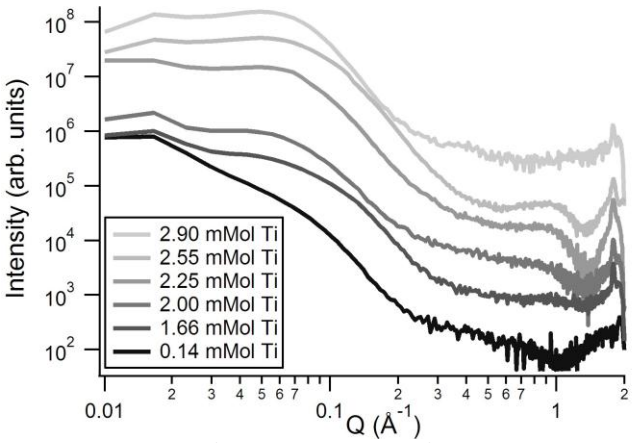

Fig. 7: SAXS patterns from powdered calcined film material recovered from the air-liquid interface after $Ti(OBu^n)_4$ concentration variation experiments using BAM.

Modelling of the data as isolated voids in a titania matrix suggests that prolate ellipsoidal holes exist in the powdered film material. The ellipsoids in calcined films have diameters of 34(±2)×62(±2)Å for $Ti(OBu^n)_4$ concentrations of 2mMol to 3mMol suggesting that the voids in the films are slightly larger than the ellipsoidal micelle cores in ethanolic FSO-100 solutions at high concentrations. When only 0.14mMol of $Ti(OBu^n)_4$ is added, however, fitting indicates that the voids have become almost rod-like at diameters of 30 x 220Å suggesting that the micelles become elongated when there is less titania present. Assuming the lamellae seen in reflectivity from *in situ* films are composed of micelles aligned near the interface, comparison with these results suggests titania wall thicknesses of 20 -30Å. At wider angles in the scattering patterns sharp peaks are observed at Q = 1.77 $Å^{-1}$, corresponding to the (101) peak of anatase suggesting the titania in the film is in this form.[31]

The porous structure suggested by SAXS experiments is supported by TEM, *Fig 8.* The images show a porous matrix of relatively large TiO_2 particles in a thick film, where only the thinner edges of the material can be successfully imaged. The images suggest that pores in the material are of the order of 100 - 200Å in diameter, which would be sufficient for the diffusion of many compounds such as photosensitive dyes used in dye sensitised solar cells. At higher magnification, *Fig 8b*, some evidence of smaller mesopores, seen in the SAXS patterns, is also visible at the thinner particle edges.

Scanning electron microscopy was used to collect secondary electron images of the surface of FSO-100 templated titania films removed onto a microscope slide and calcined. *Fig 8c* shows that most of the film remains smooth, uniform and solid although some areas have cracked and partially peeled from the substrate during drying or calcination. In the higher magnification image,

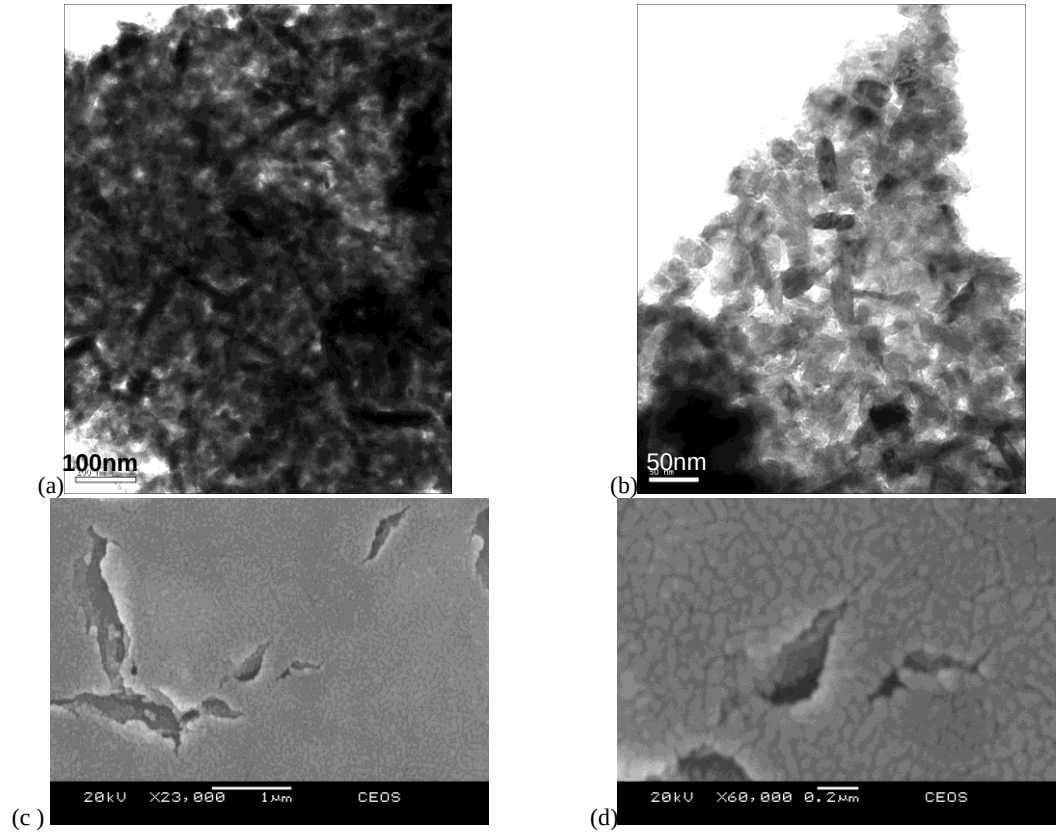

Fig. 8: Transmission electron micrographs of a titania film formed at the air-ethanol interface. Images (a) and (b) are of the edge of the film in different locations. (c), (d) Scanning electron microscope images of FSO-100 templated titania film on a microscope slide substrate.

Fig 8d, the film consists of a solid network of particles separated by 50–200Å channels again suggesting that a larger open network exists within the film. SEM also allows estimation of the film thickness; around 3 microns. (*supplementary materials*, *Fig 1S*)

Nitrogen adsorption (*supplementary materials Fig 3S*) for calcined FSO-100-templated titania films gives a Type IV isotherm with a characteristic hysteresis loop typical of mesoporous powders.[32] The BET surface area was calculated as 85 m^2g^{-1} using data in the partial pressure range of 0.06 – 0.29. This is considerably larger than the 23 m^2g^{-1} estimated by calculation of the surface area expected for randomly packed spherical voids in a titania matrix indicating the film is porous after calcination. A reliable pore-size distribution cannot be calculated from this data due to the desorption step occurring at a partial pressure of 0.4 indicating that cavitation processes, which are independent of pore size are occurring, suggestive of small pore neck sizes, but rendering the Kelvin equation assumptions invalid for this material.[33]

Discussion

FSO-100 templated titania film formation at the air-solution interface occurs gradually, over a period of hours, in Brewster angle microscopy and time-resolved X-ray reflectometry experiments. The presence of titania precursors is necessary for film formation on these solutions, but no ordered mesostructure was observed in the subphase either before or after titania precursor addition. The gradual loss of the specular peak, the growth of initially broad peaks which gain intensity and become sharper, as observed in time-resolved X-ray reflectometry, and the sustained continual development after initial film formation observed in BAM are all indicative of a gradual accumulation at the interface rather than film formation driven by aggregation of particles formed initially in the subphase.

This gradual film development is characteristic of the surface driven formation mechanism, in which individual surfactant micelles or molecular species diffuse to the surface and add to a film at the interface that continues to grow in thickness. Such mechanisms have been reported for the formation of surfactant templated silica materials at specific concentrations.[34] In that case micelle aggregation in solution prior to film formation did not occur and development of the silica film was reported to be due to individual, coated micelles adding to an initially thin film at the interface.

In the silica case, silica-coated cylindrical micelles added to the film to produce a hexagonally ordered silica-surfactant film.[34] Examination of the FSO-100 – ethanol phase diagram suggests that spherical micelles exist in the precursor solution prior to film formation (Table 1). Additionally, the observation of lamellar structures in developed films, *Fig. 6*, at the air-solution interface suggests that micelles are not adding to the surface in the manner reported for silica films. Instead it appears that either individual molecular species add to an existing lamellar phase, as has been reported for titania films in aqueous systems,[15] or that micelles adding to the film collapse and add to the lamellar phase in a more or less ordered fashion. A monolayer of fluorinated surfactant is expected to exist at the solution surface, as is well established for other surfactants at or below the critical micelle

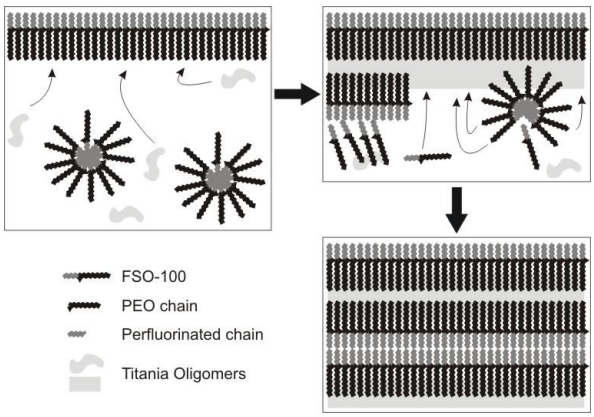

Fig. 9: Proposed formation mechanism for FSO-100 templated titania films

concentration,[35] so a surface-driven growth mechanism in the presence of titania precursors is perhaps not surprising. In the case of FSO-100 the perfluorinated section of the surfactant will be uppermost in the monolayer due to its incompatibility with the ethanol solvent and a co-operative, surface driven assembly mechanism is proposed, as shown in *Fig 9*.

For ethylene oxide based surfactants the separation, due to repulsion, between micelles is due to the entropically unfavoured overlap of PEO sections at the exterior of the micelle rather than electrostatic repulsion for ionic surfactants.[36, 37] When such surfactants are used as templates for ordered inorganic materials, the coating of surfactant micelles by inorganic precursors provides a barrier to PEO chain overlap and micelle aggregation becomes possible.[29] Interactions between growing inorganic oligomers and PEO chains, via hydrogen bonding or hydrophilic – hydrophilic interactions in the case of titania,[38] lead to the surfactant micelle becoming coated with inorganic material. Although such interactions may be in competition with water in the system, the large number of interaction sites available from inorganic oligomers leads to their strong interaction with the surfactant. However, until sufficient inorganic material is bound to the micelles to prevent PEO chain overlap the repulsive interaction will dominate, preventing aggregation in solution. The addition of an inorganic precursor, attracted to PEO, leads to the formation of a barrier between the PEO chains in the concentrated surface monolayer, enabling other surfactant monomers to attach and allowing a lamellar phase to grow downwards into solution, consisting of almost pure layers of perfluorocarbon headgroups and mixed layers of PEO and titania. Flurosurfactants are known to favour aggregation into lamellar phases and the established interactions between titania precursors and PEO chains also support the proposed mechanism.[9, 38]

This interaction between PEO chains and titania precursors is evidenced here by the decrease in film formation time observed at higher acid concentrations in BAM experiments, *Fig 3a*. Although the results of HCl and $Ti(OBu^n)_4$ variation experiments suggest that film formation occurs faster at higher for higher H_2O:Ti ratios the titania precursors are fully hydrolysed during the premixing of HCl and $Ti(OBu^n)_4$ prior to mixing with the surfactant solution. This suggests that the effect of water content on film formation time is not related to the reactions of the inorganic precursors, as does the observation that formation time decreases in spite of increased acid concentration hindering the condensation reactions of the titania.[10,11,37] However, the interactions between titania species and PEO are known to be greater if acidic water is present[38] and the greater interaction between the species at higher water contents is expected to lead to a faster coating of the PEO layer.

This increased interaction allows faster lamellar formation and so faster film formation as observed in BAM experiments. BAM results also agree with the expectation that film formation will be faster at higher surfactant concentrations as more surfactant will be readily available for the formation of each lamella, *Fig 3c*. The addition of greater amounts of $Ti(OBu^n)_4$, on the other hand, may be expected to reduce the H_2O:Ti ratio and, as a result, reduce the interaction with PEO groups leading to slower film formation as observed, *Fig 3b*. It may be expected that at sufficiently high concentrations of titania precursor the increased concentration would outweigh the effects of reduced interaction, however, this concentration was not reached in the range studied.

Although the films are confidently assigned a lamellar structure *in-situ* at the air-solution interface, the structure of dry, calcined film material removed from the interface contain a disordered porous structure from SAXS and electron microscopy studies. TEM imagees show a porous, three dimensionally structured material. The presence of a mesoporous network in calcined titania films is also supported by nitrogen adsorption and SAXS experiments where modelling shows the presence of oblate ellipsoidal voids in the crystalline titania film after calcination. Given that no lamellar phase was observed in the phase diagram of the FSO-100 surfactant at, or below, 90% wt. surfactant, Table 1, formation of a lamellar phase at the top surface of the film must be encouraged by the presence of the surfactant monolayer at the interface. Instead, at high surfactant concentrations, a high density of ellipsoidal micelles is observed in the surfactant phase diagram which bears more resemblence to the final film structure. Harvested films are much thicker than the extent of lamellar ordering indicated by the diffraction patterns, suggesting the lamellar structure is only present at the top surface of the film and the concentrated titania-surfactant phase in the majority of the film contains a disordered array of micelles. In surfactant templating concurrent inorganic condensation and micelle ordering produce a race between the development of a highly ordered material and setting of the inorganic phase into a non-malleable solid.[39, 40] Rapid condensation can limit ordering, for example, the setting of a disordered cubic phase due to an incomplete structural transition has been reported for silica powders.[39] Rapid titania condensation here may therefore limit micelle rearrangement into ordered mesophases or transformation of the entire film into a lamellar phase. After removal from the interface, surfactant structures existing in equilibrium within the wet films may also become disturbed during drying, as solvent evaporates from the film. These considerations give rise to the mesostructure observed in SAXS patterns and TEM images.

Further alteration of film structure can occur during calcination, due to crystallisation of the initially amorphous titania into anatase. At the calcination temperature used (600°C) titania crystallises forming anatase and if the growing crystals exceed the size of the pore walls this can lead to mesopore collapse.[41] The relatively thick titania-PEO walls (36Å) in these

films may help preserve mesoporosity during calcination and anatase formation, leading to formation of the network of larger titania crystals observed in the TEM micrographs, which retain some mesoporosity as observed by SAXS and nitrogen adsorption measurements.

Conclusions

Mesoporous titanium dioxide films have been formed at the air-solution interface using a partially fluorinated surfactant to direct the structure and using minimal water reaction conditions to slow the inorganic polymerisation. Film formation is found to be dependent upon the water to titania ratio in the reaction solution, which determines the extent of the interaction between the PEO headgroup of the surfactant and the growing titania oligomers. Film formation has also been achieved with the complete absence of water in the reaction solution, the first time to our knowledge this has been achieved in standard laboratory conditions. The films are observed to be porous on a 10 nm scale by transmission electron microscopy, while SAXS demonstrates retention of 34×62Å diameter mesopores after calcination at 600°C. This hierarchical porosity is ideal for applications needing rapid diffusion into a material, coupled with a high surface area for active sites, such as required for photocatalysis or dye sensitised solar cells. Applications of these films are now being pursued.

Acknowledgments

We would like to thank DuPont for the kind donation of the FSO-100 surfactant. We also acknowledge the European Synchrotron Radiation Facility for provision of synchrotron radiation facilities and we would like to thank Dr O. Konovalov for assistance in using beamline ID10B. We thank Dr P. Taylor for assistance with neutron reflectivity experiments on SURF (experiment RB720049) and Dr S. King for assistance with SANS experiments on LOQ (experiment RB620142) at ISIS. We also thank Dr J. Mitchels and Dr U. Potter from the Centre for Electron Optical Studies at the University of Bath for assistance with TEM and SEM data collection. Dr S. Rigby (Nottingham) is thanked for helpful discussions on nitrogen adsorption. A.M.H. also acknowledges funding from the ORSAS scheme at the University of Bath.

Notes and references

[a] *Department of Chemistry, University of Bath, Claverton Down, Bath, BA2 7AY, UK. Fax: +44 1225 386231; Tel: +44 1225 384192; E-mail: k.edler@bath.ac.uk*

[b] *present address: Australian Synchrotron, 800 Blackburn Rd, Clayton, Victoria 3168, Australia. Fax: +61 3 8540 4200; Tel: +61 3 8540 41; E-mail: Adrian.Hawley@synchrotron.org.au.*

1. J. S. Beck, J. C. Vartuli, W. J. Roth, M. E. Leonowicz, C. T. Kresge, K. D. Schmitt, C. T.-W. Chu, D. H. Olson, E. W. Sheppard, S. B. McCullen, J. B. Higgins and J. L. Schienker, *J. Am. Chem. Soc.*, 1992, **114**, 10834-10843.
2. G. d. A. Soler-Illia, C. Sanchez, B. Lebeau and J. Patarin, *Chem. Rev.*, 2002, **102**, 4093-4138.
3. A. Corma, *Chem. Rev.*, 1997, **97**, 2373-2419.
4. M. Zukalova, A. Zukal, L. Kavan, M. K. Nazeeruddin, P. Liska and M. Gratzel, *Nano Letters*, 2005, **5**, 1789-1792.
5. L. Zhao, Y. Yu, L. Song, X. Hu and A. Larbot, *Appl. Surf. Sci.*, 2005, **239**, 285-291.
6. P. Innocenzi, A. Martucci, M. Guglielmi, A. Bearzotti and E. Traversa, *Sensors Actuators B*, 2001, **76**, 299-303.
7. E. Kissa, *Fluorinated Surfactants and Repellents*, Marcel Dekker Inc., New York, 2001.
8. H. Hoffmann and J. Wurtz, *J. Mol. Liq.*, 1997, **72**, 191-230.
9. J. Ravey, M. Stebe, S. Sauvage and C. Elmoujahid, *Colloids Surf. A*, 1995, **99**, 221-231.
10. Y. Di, X. Meng, S. Li and F.-S. Xiao, *Microporous Mesoporous Mater.*, 2005, **82**, 121-127.
11. J. Blin, P. Lesieur and M. Stebe, *Langmuir*, 2004, **20**, 491-498.
12. X. Meng, Y. Di, L. Zhao, D. Jiang, S. Li and F.-S. Xiao, *Chem. Mater.*, 2004, **16**, 5518-5526.
13. P. Innocenzi, L. Malfatti, T. Kidchob and P. Falcaro, *Chemistry of Materials*, 2009, **0**.
14. M. J. Henderson, A. Gibaud, J.-F. Bardeau and J. W. White, *J. Mater. Chem.*, 2006, **16**, 2478-2484.
15. M. J. Henderson, D. King and J. W. White, *Langmuir*, 2004, **20**, 2305-2308.
16. Edler, Karen J., A. M. Hawley, B. M. D. O'Driscoll and R. Schweins, *Chem. Mater.*, 2010, **22**, 4579-4590.
17. C. J. Brinker and G. W. Scherer, *Sol-Gel Science*, Academic Press, London, 1990.
18. C. Sanchez and J. Livage, *New J. Chem.*, 1990, **14**, 513-521.
19. D.-M. Smilgies, N. Boudet, B. Struth and O. Konovalov, *J. Synchrotron Radiation*, 2005, **12**, 329–339.
20. K. Edler, A. Goldar, A. V. Hughes, S. J. Roser and S. Mann, *Microporous Mesoporous Mater.*, 2001, **44**, 661-670.
21. A. Nelson, *J. Appl. Cryst.*, 2006, **39**, 273-276.
22. J. Penfold, R. M. Richardson, A. Zarbakhsh, J. R. P. Webster, D. G. Bucknall, A. R. Rennie, R. A. L. Jones, T. Cosgrove, R. K. Thomas, J. S. Higgins, P. D. I. Fletcher, E. Dickinson, S. J. Roser, I. A. McLure, A. R. Hillman, R. W. Richards, E. J. Staples, A. N. Burgess, E. A. Simister and J. W. White, *J. Chem. Soc., Faraday Trans.*, 1997, **93**, 3899-3917.
23. R. K. Heenan, J. Penfold and S. M. King, *J. Appl. Cryst.*, 1997, **30**, 1140-1147.
24. S. R. Kline, *J Appl. Cryst.*, 2006, **39**, 895.
25. P. Yang, D. Zhao, D. I. Margolese, B. F. Chmelka and G. D. Stucky, *Nature*, 1998, **396**, 152-155.
26. P. D. Yang, D. Y. Zhao, D. I. Margolese, B. F. Chmelka and G. D. Stucky, *Chem. Mater.*, 1999, **11**, 2813-2826.
27. D. Grosso, G. d. A. Soler-Illia, F. Babonneau, C. Sanchez, P. Albouy, A. Brunet-Bruneau and A. R. Balkenende, *Adv. Mater.*, 2001, **13**, 1085-1090.
28. G. S. Attard, J. C. Glyde and C. G. Goltner, *Nature*, 1995, **378**, 366-368.
29. C. Fernandez-Martin, K. J. Edler and S. J. Roser, *J. Mater. Chem.*, 2008, **18**, 1222 - 1231.
30. K. Edler, A. Goldar, T. Brennan and S. J. Roser, *Chem. Commun.*, 2003, **14**, 1724-1725.
31. P. Angerer, L. G. Yu, K. A. Khor and G. Krumpel, *Mater. Sci. Eng. A*, 2004, **381**, 16-19.
32. S. J. Gregg and K. S. W. Sing, *Adsorption, Surface Area and Porosity*, Academic Press, New York, 1982.
33. M. Thommes, B. Smarsly, M. Groenewolt, P. I. Ravikovitch and A. V. Neimark, *Langmuir*, 2006, **22**, 756-764.
34. T. Brennan, A. V. Hughes, S. J. Roser, S. Mann and K. J. Edler, *Langmuir*, 2002, **18**, 9838-9844.
35. E. M. Lee, R. K. Thomas, J. Penfold and R. C. Ward, *J. Phys. Chem.*, 1989, **93**, 381-388.
36. K. Flodström, H. Wennerström and V. Alfredsson, *Langmuir*, 2004, **20**, 680-688.
37. J. D. Epping and B. F. Chmelka, *Curr. Op. Colloid Interface Sci.*, 2006, **11**, 81-117.
38. G. J. A. A. Soler-Illia and C. Sanchez, *New J. Chem.*, 2000, **24**, 493-499.
39. K. Flodström, H. Wennerström, C. V. Teixeira, H. Amenitsch, M. Lindén and V. Alfredsson, *Langmuir*, 2004, **20**, 10311-10316.
40. G. J. d. A. A. Soler-Illia, E. L. Crepaldi, D. Grosso and C. Sanchez, *Curr. Op. Colloid Interface Sci*, 2003, **8**, 109-126.
41. E. L. Crepaldi, G. J. de A. A. Soler-Illia, D. Grosso and C. Sanchez, *New J. Chem.*, 2003, **27**, 9 - 13.